Engineering Geology xxx (xxxx) xxx–xxx

Contents lists available at ScienceDirect

Engineering Geology

journal homepage: www.elsevier.com/locate/enggeo

Detection and characterization of animal burrows within river embankments by means of coupled remote sensing and geophysical techniques: Lessons from River Panaro (northern Italy)

Lisa Borgatti[a], Emanuele Forte[b,c,*], Arianna Mocnik[b,c], Roberta Zambrini[c], Federico Cervi[a], Davide Martinucci[b,c], Federica Pellegrini[d], Simone Pillon[b,c], Alessandro Prizzon[c], Andrea Zamariolo[c]

[a] University of Bologna, Department of Civil, Chemical, Environmental and Materials Engineering DICAM, Viale Risorgimento 2, 40136 Bologna, Italy
[b] University of Trieste, Department of Mathematics and Geosciences, Via Weiss 1, 34128 Trieste, Italy
[c] Esplora srl, Spin-Off University of Trieste, Via Weiss 1, 34128 Trieste, Italy
[d] Agenzia Interregionale per il fiume Po - AIPo, Via Fonteraso 15, 41100 Modena, Italy

ARTICLE INFO

Keywords:
Flood control structures
Flood risk
Animal burrows
Piping
Geophysics
Subsurface imaging

ABSTRACT

The damage and the eventual breach of river embankments may be due to internal erosion and instability processes in the waterside and landside slopes. Beside the progressive degradation of soil properties, different types of macro-pores inside the levee body can influence its short- and long-term performance. Among macro-pores, burrows are a widespread form of biologic erosion of earthen structures potentially producing damage or even their collapse. In fact, animal burrows are erosion tunnels, which can lead to piping phenomena. Thus, the emergent risk connected to burrowing animals in earthen levees has to be tackled, given also the environmental changes driven by human activity and climate. Remote sensing and geophysical surveys can complement data from in situ investigation campaigns in the definition of the real-embankment model, as well as in the imaging of local defects which may influence its local and/or global stability. Several techniques were integrated in the study area of the Panaro River, where an active animal burrow was detected in spring 2015. Two campaigns were carried out: Survey-1, in June 2015, just after the relocation of the animals, and Survey-2 in December 2015, after the filling of the burrow with a cement-bentonite slurry. Here, we highlight the peculiarity of each method and the choice of an integrated multi-technique approach. The results allowed the known burrow, as well as two other tunnels, to be imaged in 3D, providing specific guidelines for the best integrated strategy to detect and characterize these macro-pores in a fluvial levee. The proposed approach can advance our knowledge of embankments in space and time, so that effective remedial actions in flood risk and wildlife management can be identified.

1. Introduction

Several scenarios or chain of events can lead to the progressive deterioration, the damage, and the breach of river embankments, which may be due to internal erosion and instability processes in the waterside and landside slopes (FEMA, 2005).

Beside the progressive degradation of soil properties, different types of macro-pores inside the levee body can influence its short- and long-term performance. Macro-pores are generally represented by cracks and fissures in the dike body due to natural consolidation and shrinking-swelling processes, to human and animal activity and to the presence of vegetation. Macro-pores may influence the performance of river embankments by increasing rainfall infiltration and inducing preferential and eventually deeper groundwater flow paths and irregular saturation degree. When the water level in the nearby channels increases, the heterogeneity due to the presence of macro-pores influences the final pore pressure distribution. If the pore water pressures would increase, the effective stresses and the shear strength would be reduced and macro-instability could eventually occur. Moreover, if the macro-pores somehow connect the two sides of the levee, the internal erosion can be accelerated until failure eventually takes place (FEMA, 2005; CIRIA, 2013).

Among macro-pores, burrows are a widespread form of biologic erosion of earth levees, embankments and dams that lead to an

* Corresponding author at: University of Trieste, Department of Mathematics and Geosciences, Via Weiss 1, 34128 Trieste, Italy.
E-mail address: eforte@units.it (E. Forte).

http://dx.doi.org/10.1016/j.enggeo.2017.06.017
Received 3 March 2017; Received in revised form 8 May 2017; Accepted 24 June 2017
0013-7952/ © 2017 Elsevier B.V. All rights reserved.

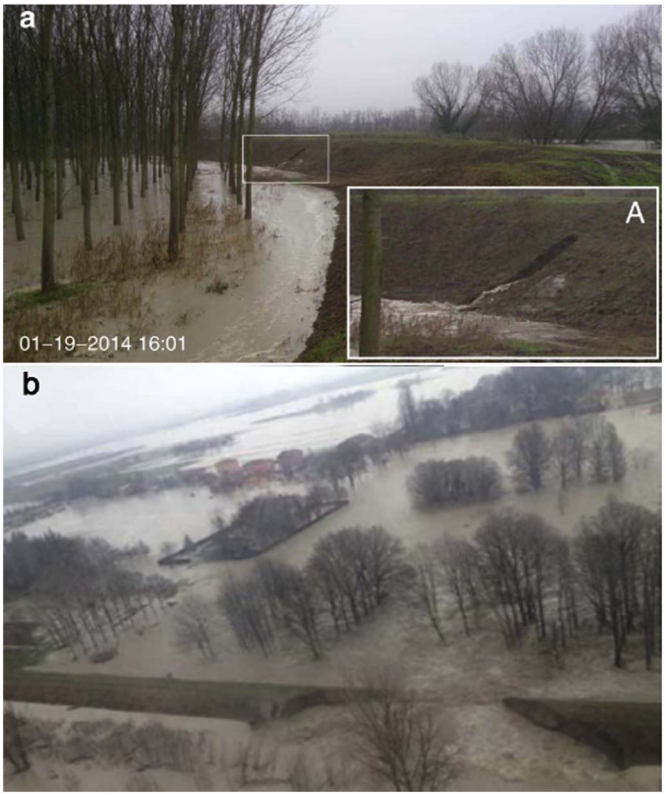

Fig. 1. a) Breach and b) failure of Secchia River embankments during the 19th January 2014 flood (after Orlandini et al., 2015 – a; D'Alpaos et al., 2014 – a, b).

increased risk during flooding events potentially producing structure damage or even its collapse. In fact, animal burrows are erosion tunnels, which can lead to piping phenomena; piping is in turn responsible to approximately half of the world's dam failures (Richards and Reddy, 2010). Moreover, Orlandini et al. (2015) and Taccari (2015) have recently shown how earthen levees disturbed by burrowing animals may fail causing disastrous floods, and have documented a possible animal-induced levee failure mechanism (Fig. 1, D'Alpaos et al., 2014; Orlandini et al., 2015). Besides these recent papers, case studies generally deal with management and maintenance issues, while relatively few studies were carried out to quantitatively assess the biological damage in earthen structures (Bayoumi and Meguid, 2011). Thus, the emergent risk connected to burrowing animals in earthen levees has to be tackled given also the environmental changes driven by human activity and climate (Orlandini et al., 2015).

In order to detect and characterize earthen structures disturbed by animal burrows, the pieces of information from direct, but punctual, investigation and monitoring campaigns must be complemented with indirect, but distributed, data from geophysical surveys, which can help in the definition of the real-embankment model with local punctual/linear/areal anomalies acting as defects which may influence its overall stability on the short- and long-term.

Several geophysical techniques have been applied on embankments and levees with different purposes. Most of the examples are related to imaging the internal structure and estimate the main stratigraphic and hydrogeological features (Panthulu et al., 2001; Cho and Yeom, 2007; Niederleithinger et al., 2012; Perri et al., 2014; Busato et al., 2016; Loperte et al., 2016). Some other papers focus on the detection of voids within the levee structure. In detail: Butler et al. (1994) applied resistivity and magnetic measures to detect badger burrows; Sheng Huoo et al. (2002) investigated the capability of GPR to detect voids with different size by means of laboratory tests; Kinlaw et al. (2007) analyzed the ability of GPR to find tortoise nests; Xu et al. (2010) used the same technique to detect subsurface voids inside dikes and dams. Di Prinzio et al. (2010) proposed the GPR as a standalone tool to detect burrows; Sentenac et al. (2012), as well as Jones et al. (2014) applied 2D and 3D resistivity measurements (ERT) to locate fissures in embankments, while Chlaib et al. (2014) and Samyn et al. (2014) considered the affordability of GPR in discriminating voids from water-filled cavities or metallic objects.

From the previously cited literature we can infer that the geophysical techniques most tested for the problem under examination are ERT and GPR, while some other methods are seldom reported to detect voids, not necessarily in river embankments, like gravimetry (e.g. Butler, 1984) and reflection seismic (e.g. Branham and Steeples, 1988; Deidda and Ranieri, 2005; Lorenzo et al., 2014). Thermal imagery has been proposed as a safety tool for detecting dam seepage (e.g. Deitchman and Loheide II, 2009) but no applications have been exploited to detect voids within flood control structures.

From the geophysical point of view, the detection of a "void" (i.e. any air-filled volume) in the subsurface is based on its physical contrast with the surrounding material. Such a contrast is very high for several physical parameters like density, electrical conductivity, electrical permittivity, seismic velocity. Each specific geophysical technique has its own advantages and disadvantages depending not only on the physical contrast, but, often equally important, on logistical issues, on achievable resolution, on target geometry and depth.

Remote sensing and several geophysical techniques were integrated in the study area of the Panaro River, where an active animal burrow was detected in spring 2015. In this area, two campaigns were carried out: Survey-1, in June 2015, just after the relocation of the animals, and Survey-2 in December 2015, after the complete filling of the burrow with cement-bentonite slurry. In the following sections we briefly highlight the peculiarity of each method, giving reason to our choice of an integrated multi-technique approach. The results allowed to image in 3D the known burrow as well as two others, providing specific guidelines for the best integrated strategy to detect and characterize such kind of structures in a fluvial levee. The proposed approach can advance our knowledge of embankments in space and time, so that effective remedial actions in flood risk and wildlife management can be identified.

2. Study site

We selected a portion on the inner flank of left levee of the Panaro River, where a European badger burrow was previously detected (Figs. 2 and 3c).The River Panaro is a water course tributary of the Po River (northern Italy) having a length of about 150 km and flowing in the Emilia-Romagna Region. The total catchment area is 1784 km^2, with mean annual precipitation of about 1017 mm. It flows through the central section of the northern Apennines down to the Po Plain. Upstream, the catchment is formed by a hilly zone, with sandstones and clayey marls, while downstream recent alluvial deposits outcrop. After the 1950s, in fact, a series of hydraulic works were carried out to reclaim plain areas and the River is now an almost artificial watercourse for long sectors of its course (Castaldini and Ghinoi, 2008).

In the study area, the present-day geometry of the embankment derives from subsequent enlargements of historical levees dating back to 4th–5th century A.D. The most recent works in this sector were carried out after the breach of Malpasso di Cà Bianca (11th November 1982, Fig. 2). Stratigraphic and lithological characteristics from the two boreholes are somehow variable, but the evidence of two or more levee bodies of different age and compaction was not found. Starting from the top of the levee (around 23 m above sea level - asl) 3 main units can be recognized. Unit 1 forms the top of the levee ad comprises layers of clayey silt and gravels. The levee body is composed by silt with sand (Unit 2). Underneath, Unit 3 is composed by clayey silt alternating with sand with silt in sub-horizontal layers and can be considered the natural soil at the base of the embankment.

Water table or partial saturation was found at − 8 m from the top of

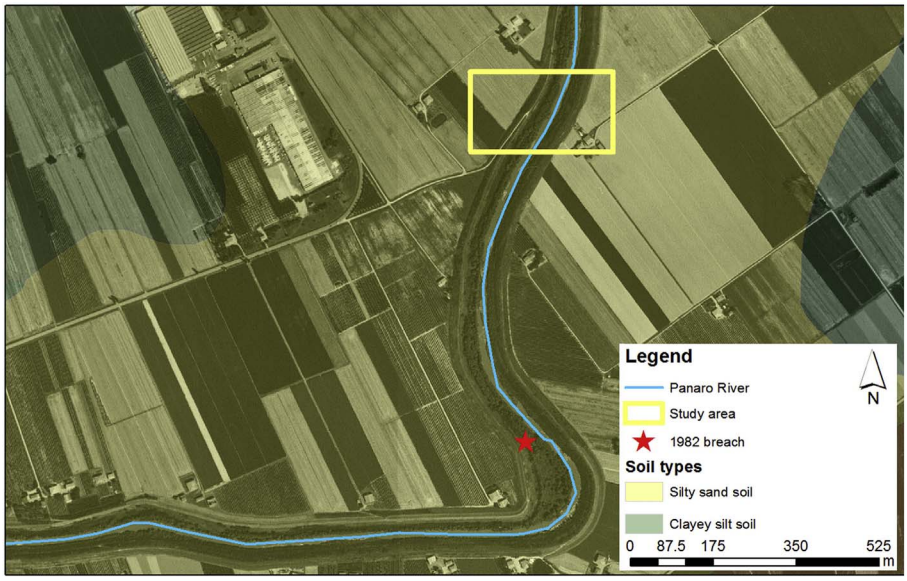

Fig. 2. Location of the study area with the position of the 1982 breach and the lithology of outcropping soils.

the levee, that is 15 m asl, which corresponds to the calculated elevation of the water in the river at the time of the surveys (15.2 m asl at Camposanto gauge station, 12 km upstream, that is a local level of 13.8 m asl considering a 12 cm/km gradient). Thus, at that time, the groundwater table in the local phreatic aquifer and the river were in equilibrium.

After the disastrous flood caused by the collapse of the right embankment of the Secchia River occurred in January 2014 (D'Alpaos

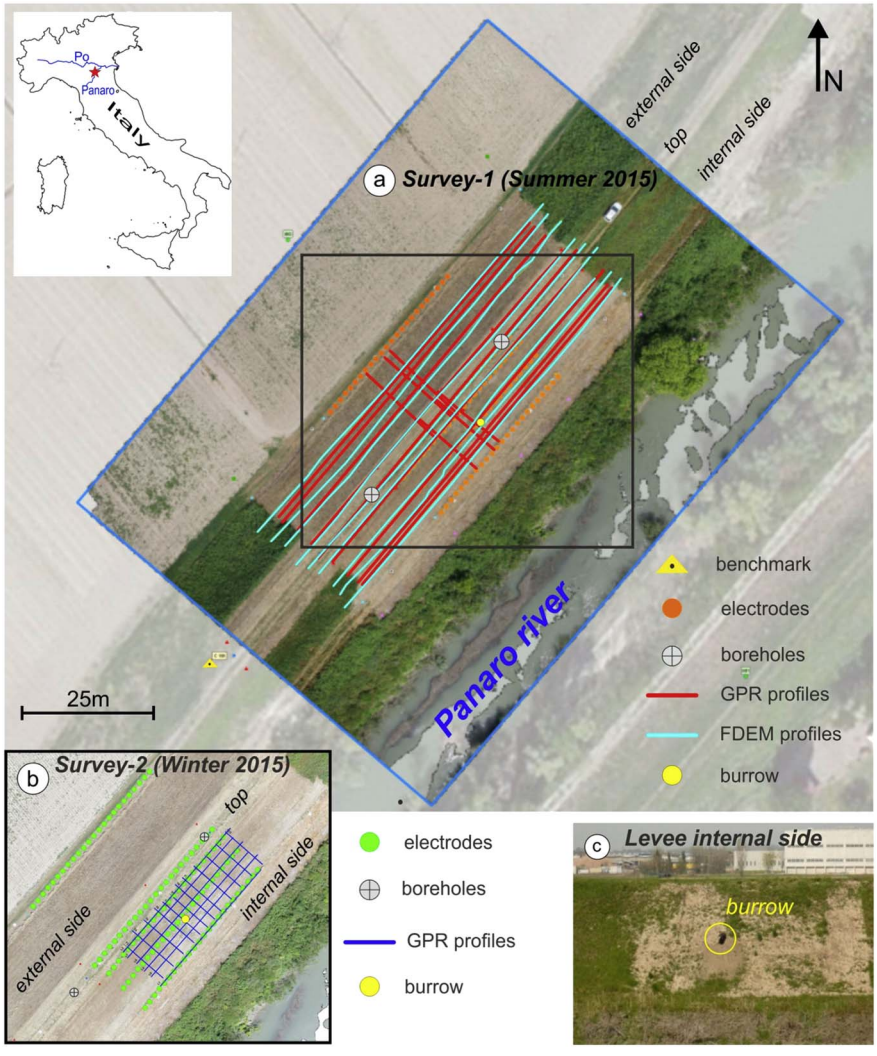

Fig. 3. Location maps of the study area extracted from the GIS showing the location of the known badger burrow entrance, the geophysical surveys, and the positions of the boreholes. a) Map of Survey-1 (Summer 2015); b) Map of Survey-2 (Winter 2015); c) Picture of the internal flank of the levee (Summer 2015) with the location of the known burrow entrance.

et al., 2014; Orlandini et al., 2015), along the main river courses in this sector of the alluvial plain including the Panaro River, 1700 critical points were detected. Interventions were planned in almost 800 animal burrows, mainly filling of the cavities with loose earthen materials and placing steel nets. Based on the evidence of the emerging risk associated with embankment failure as a consequence of animal burrows (Orlandini et al., 2015), a specific wildlife management plan was started. From January 2016, a total of 3 European badgers and 18 porcupines were caught and delocalized in the vicinity of the study area. The number of foxes and coypu caught in a larger sector of the plain is in the order of one thousand per year (AIPo, personal communication).

3. Materials and methods

On a portion of the western levee of the Panaro River two surveys (Fig. 3a, b) were carried out in four days on June 2015 (Survey-1) and in two days on December 2015 (Survey-2). Survey-1 objectives were to compare and evaluate the effectiveness of different methods to detect burrows and image their shape below the surface with environmental and logistical conditions typical of most of the levees in the Po plain. Survey-2 focused on a portion of the previously investigated area (Fig. 3b) and was done after a restoration activity (November 2015) during which the burrow was filled by about 19 m^3 of bentonite cement and a reshaping of the levee was performed.

Based on the geometrical and geological features of the earthen embankment, and considering the shape, the dimensions and the depth of the targets, a number of remote sensing and geophysical techniques have been tested. Before the geophysical measurements we surveyed the entire area with a Neutech NT4C Unmanned Airborne Vehicle (UAV), equipped with a Sony NEx7 photocamera, obtaining orthophotos with an overall resolution at the ground equal to 0.02 m, allowing to reconstruct a detailed Digital Surface Model (DSM) of the embankment by means of Aero-Photogrammetric (APT) Techniques (Cannarozzo et al., 2012). An accurate DSM is in fact essential in order to evaluate both the actual geometry of the levee and to position the subsurface targets accurately. We used a differential double-frequency (L1/L2) topographic GPS in RTK mode (model GNSS Stonex S9III, with RTK L1/L2 receiver having 220 channels) to collect high precision measures of 12 target locations (white plastic squares with high contrast black patterns, having a 0.5 m long side), which are essential in the APT technique to calibrate and properly combine and mosaic the pictures taken by the UAV (Cannarozzo et al., 2012). Moreover, the GPS was used to positioning natural (the burrow entrance, some stones at the surface) and man-made elements (datum and reference points, the borders of the levee), as well as the acquisition points of the geophysical surveys.

In Survey-1 we integrated Infrared Radiation (IR) pictures, Electrical Resistivity Tomography (ERT), Frequency Domain Electro-Magnetic (FDEM), and Ground Penetrating Radar (GPR) measurements (Fig. 3a), while Survey-2 encompassed only ERT and GPR techniques (Fig. 3b).

3.1. Remote sensing and geophysical surveys: methods and acquisition survey design

3.1.1. IR survey

We used a Flir T335 IR thermocamera with a thermal sensitivity of 50 mK, mounted above the ground surface on a dedicated tripod. A total of 80 combined IR and visible picture pairs have been collected in the study area both on the external and internal side of the levee. 45 images have been taken from 10.30 a.m. to 16 p.m., while the other 35 in the following night from 10 p.m. to 1 a.m. This way it is possible to detect thermal anomalies both colder and warmer than the mean temperature, by exploiting the thermal capacities of materials like air, dry and wet soil, vegetation, and so on (e.g. Anderson, 2005). During data collection, approximately every hour, the mean external temperature and the relative humidity have been recorded in order to better constrain the processing of the IR data. The external temperature had a range from 25 °C at 10.30 a.m. to 31 °C at 16 p.m., having an almost constant value of 21 °C during the night; the relative humidity in the same time intervals spanned from 53% to 34% during the day, being always close to 56% during the nighttime measurements.

3.1.2. GPR

GPR is a pulsed electromagnetic technique designed to detect electrical discontinuities beneath the earth's surface (e.g. Daniels, 2004; Jol, 2009). The basic and most common systems are composed of a couple of transmitting and receiving antennas, which are respectively used to emit and record ultra-wide-band electromagnetic radiation and to detect its reflections from buried targets. Arrival time and amplitude of such reflections are exploited to image dielectric discontinuities, which in turn are related to materials having different electrical characteristics. The formal equivalence of elastic and electromagnetic wave propagation in horizontally layered media established by Ursin (1983) allows data analysis and processing with algorithms originally developed for exploration seismology techniques. The maximum penetration depth depends by several factors like: central frequency of the emitted EM pulse, lithology, water content, texture, and grain size, being the best conditions low conductive compact materials investigated by relatively low frequencies. A rough estimation of the maximum achievable investigation depth (Z_{max}) in a low conductive medium can be obtained by using the relation (Daniels, 2004):

$$Z_{MAX} = \frac{\sqrt{\varepsilon_r'}}{60\pi\sigma'} \quad (1)$$

In which ε_r' is the real part of the relative electric permittivity (dimensionless) and σ' is the real part of the electric conductivity (Sm^{-1}).

The vertical resolution is proportional to the used frequency band, while the horizontal resolution is primarily depending by the trace interval (lateral sampling) but also by the frequency being inversely proportional to the depth of the target, as for any other geophysical technique. Therefore a trade-off between the maximum investigation depth and the desired resolution level must always be made.

For both surveys we used a Zond-12 GPR system, equipped with a 300 MHz shielded bi-static antenna pair. The shielding box was mounted on a dedicated plastic device with three wheels allowing an easier movement on the flanks of the embankment. A support for the GPS antenna was further mounted above the center of the antenna to achieve in real time an accurate positioning of the acquired measurements.

We used an electromechanical odometer to trigger the instrument every 0.05 m, recording 512 samples per trace, with a sampling interval of 586 ps; so the recording time window was fixed at 300 ns. The vertical stacking was equal to 16. All the reported acquisition parameters have been used for both Survey-1 and Survey-2.

A total of 12 profiles have been collected during Survey-1: 9 longitudinal (3 on the levee top, 3 on the internal and other 3 on the external side) and 3 transversal (Fig. 3a) reaching a total length of about 790 m. Survey-2 encompassed 18 profiles, all in the inner portion of the levee: 6 longitudinal and 12 transversal (Fig. 3b) reaching a total length of about 320 m.

All the data has been processed with the same flow including: DC removal, drift removal (zero time correction), geometrical spreading correction, exponential amplitude correction, bandpass filtering, velocity analysis on diffraction hyperbolas, depth conversion, topographic (static) correction, and 2D migration (Kirchhoff). We further evaluated the effect of tilting corrections (Forte and Pipan, 2009), but considering the approximation of the applied velocity field and the limited penetration depth of GPR signal we deemed such correction not essential for this specific case. In fact, considering a mean dip of the embankment

equal to 30° and a depth of 1.5 m the maximum error in the trace location due to the tilting of the antenna would be of about 35 cm. Specific analysis techniques based on GPR attribute analysis (e.g. Forte et al., 2012; Zhao et al., 2013) have been further applied in particular to highlight possible peculiar characteristics of the burrow in terms of phase and frequency signature. All the available data was combined into a single pseudo 3D dataset by using Petrel® software, giving to each trace its actual spatial location and allowing a more straightforward link and integration in a Geographic Information System (GIS) with results obtained by the other methods.

3.1.3. ERT

ERT is based on the injection of a measured electric current at a certain measured voltage to evaluate the distribution of the electrical resistivity in the subsurface. The ERT technique requires a galvanic contact with the survey so producing measures related to a previously fixed geometrical configuration. We used an IRIS Syscal Pro georesistivimeter connected to 72 electrodes. A 3D geometry was selected in order to cover both the internal and the external sides of the levee and to obtain high quality data. A full dipole-dipole geometry was adopted acquiring two originally separated datasets each of them having 4014 apparent resistivity measurements. Such data was then combined together and inverted as a single dataset. The electrode spacing was set equal to 1.5 m. In Survey-2 we relocated the electrodes as in Survey-1, precisely repeating the same acquisition geometry. The data were acquired both in direct and in reciprocal mode, reversing the current and potential electrodes for each measurement at least three times in order to make possible an estimation of the measurements errors and, by a stacking procedure, to minimize random noises.

For the data analysis and inversion we used the ERTLab suite (Multi-Phase Technology and Geostudi Astier), which is based on tetrahedral finite elements and manages any 3D dataset, even acquired on a complex topographic surface. After a data quality check and selection, considering both reciprocal measurements, thresholds on the minimum current and voltage, as well as on the maximum percentage RMS error limited at 3%, we inverted the whole dataset by using a smoothness constrained least-squared algorithm. The obtained “true” resistivity models can be visualized in 3D or sliced in any direction so allowing a detailed subsurface analysis.

3.1.4. FDEM

This method is one of the so-called low frequency electromagnetic techniques, which encompass a wide range of applications and instruments (Reynolds, 1997). We used a frequency domain single frequency, near field, active instrument, namely the DUALEM-642s. It works with a single transmitting coil producing a primary magnetic field having a frequency equal to 9.1 kHz and inducing a secondary current into the ground. Three pairs of coils perpendicular to each other are located at three different and constant offsets from the transmitting one. This way three coils are co-planar (HCP) and the three other are perpendicular (PRP) to the transmitter. The HCP coils are focused on the changes in electrical conductivity close to the surface, while PRP coils are more sensitive to deeper, relatively low conductive structures. The maximum depth from which it is possible to obtain reliable data in terms of sufficiently high signal-to-noise ratio is in the range of 0.5–1 times the skin depth (δ), being the latter the distance at which the amplitude of a signal propagating in an homogeneous and isotropic half-space is reduced by a factor equal to 1/e (i.e. about 37%) and it can be estimated as (Reynolds, 1997):

$$\delta \cong \sqrt{\frac{2}{\omega \mu_0 \sigma}} \tag{2}$$

where ω is the angular frequency ($2\pi f$), σ the DC electric conductivity and μ_0 the magnetic permeability of the free space. The penetration depth is also a function of the offset between the coils (keeping constant the frequency); in the used instrument the maximum depth reached with high enough signal-to-noise ratio is about 6 m below the surface, obviously decreasing when high conductive materials lie close to the topographic surface.

The used instrument is able to simultaneously measure and store 6 conductivity values (i.e. two couples for each of the three offsets) also keeping values of pitch and roll of the instrument. DUALEM instruments operate by electromagnetic induction, so no contact with the ground is needed, but considering the dimensions of the equipment (total length of 6.4 m) and its weight, we put it into a dedicated plastic device with ropes to move the entire equipment in a safe a controlled way also along the dipping sides of the levee. During the data acquisition, with a set time triggering equal to 1 s (and equivalent to the RTK GPS directly tie to the end of the EM device) we checked the roll trying to minimize the acquisition of measures having roll values exceeding ± 10°, which in any case have been removed during the following data quality control.

We acquired 9 profiles parallel to each other of which: 3 on the top and 6 on the internal flank of the levee, almost along the same paths of the GPR profiles (Fig. 3a).

The FDEM profiles have been processed with EM4soil software (Emtomo Lda) with the following flow:

- GPS FDEM data link and geometry assessment
- Data quality control (pitch, roll, and topography), affordability thresholds definition and filtering
- Initial model setting and 2D data inversion
- Evaluation of the models by means of RMS values and DOI index.

The inversion was based on a non-linear smoothness-constrained (Monteiro Santos, 2004) algorithm, which uses a terrain model made by a series of 1D models geometrically distributed as a function of the real measurement positions. The software encompasses two different implemented modeling routines, of which one based on the cumulative behavior (McNeill, 1980) and the other based on the full solution of the Maxwell equations (Kaufman and Keller, 1983).

In order to quantitative evaluate each obtained model we considered both the RMS cumulative error, which gives the reliability of the model from the mathematical point of view but cannot assure the “geological” meaningfulness, and the DOI (depth of investigation index, Oldenburg and Li, 1999). The latter represents a measure of the affordability of the inverted results as a function of the sensitivity of the reference conditions, by comparing the calculated conductivity (σ) with different starting conditions (σ^{REF}). It is defined as:

$$I_{DOI} = \left| \frac{\sigma_2(z) - \sigma_1(z)}{\sigma_2^{REF}(z) - \sigma_1^{REF}(z)} \right| \tag{3}$$

I_{DOI} values closer to zero mean that the inversion results are quite affordable because the inversion is almost independent by the starting conditions.

Beside the 2D inversion we also applied a pseudo-3D inversion algorithm based upon the Occam's regularization method on the dataset obtained by combining all the FDEM 2D profiles (Monteiro Santos et al., 2011). From the pseudo-3D inverted volume it is possible to obtain and analyze slices made in any direction, even if with different resolution levels, which can be useful to better image the shape of specific structures or targets like, in our case, a burrow.

3.2. Boreholes, sampling and lab analyses

In order to define the stratigraphy and the soil properties, field and laboratory tests were performed. Two boreholes were drilled on the embankment, reaching 10 m depth (SCC 199 + 45 and SCC 199 + 84, Fig. 3). Three disturbed core samples have also been collected and standard laboratory tests have been performed to appraise eventual

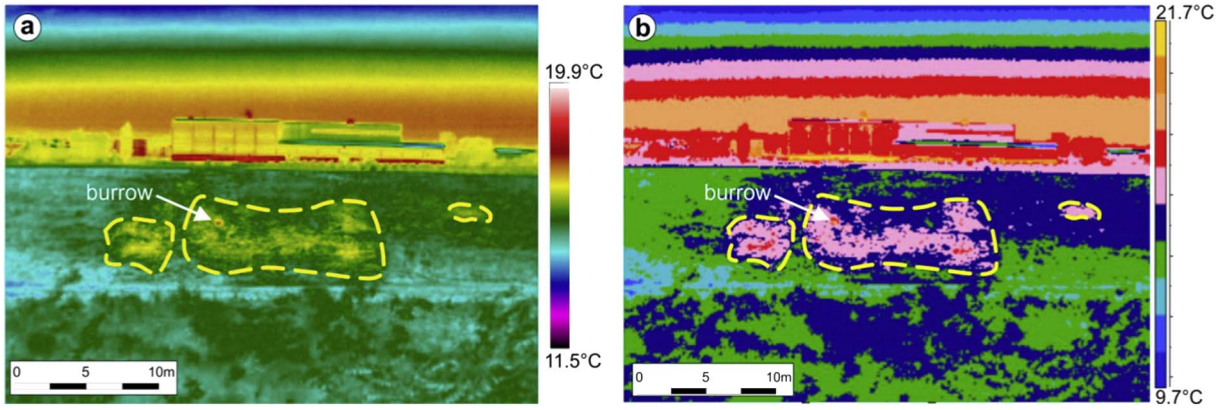

Fig. 4. IR pictures taken during Survey-1: a) nighttime image, b) daytime image. The dashed yellow line marks on both pictures zones warmer than the surrounding. (For interpretation of the references to colour in this figure legend, the reader is referred to the web version of this article.)

spatial differences in mechanical and hydrogeological properties along the levees (CR1 2–2.6 m; CR2 3.4–4 m; CR3 5–5.5 m): particle size analysis (hydrometer and sieve analysis); unit weight γ; liquid and plastic Atterberg limits; permeability.

4. Results from coupled remote sensing and geophysical techniques

4.1. Remote sensing

The IR pictures have evidenced some features that could be ascribed to the internal prosecution of the burrow, or linked to internal structure of the Panaro embankment. Generally, during the daylight, the burrow is characterized by lower temperature respect the surrounding material, due to the warming up by the sun. In the night, we can observe a contrary behavior. The higher thermal gradient is better achievable during the night. The picture taken of the internal side in the night at about 11 p.m. (Fig. 4a) shows that the burrow is characterized by higher temperature (red point, T_{MAX} equal to 18.5 °C) respect those of the surroundings. Both on nighttime and daytime images different areas thermally warmer have been depicted: they can be produced by different combined effects namely: the presence of galleries inside the embankment, paths of animals close to the burrows entrance, surface digging made by animals. Some of the warmest points inside the dashed area can be further interpreted as other burrow entrances (see also in the discussion section) or as air-filled tunnels very close to the topographic surface. Similar situations have been evidenced also in other parts of the surveyed area.

4.2. GPR

The high electromagnetic impedance contrast due to the presence of "voids" or more precisely of air-filled cavities should produce evident amplitude reflections or diffractions depending by the size of the cavity, which produces a diffraction when its size is approximately equal to the dominant wavelength of the transmitted electromagnetic signal (e.g. Jol, 2009). In Fig. 5a 3D view of some of the GPR processed profiles is provided. The mean achieved penetration depth is of about 1.5–2 m. Considering a mean velocity of 0.10 m/ns, calculated for Survey-1 by means of diffraction hyperbola analyses, and approximating the subsurface as a low-loss material ($\sigma < 1 \times 10^{-2}$ Sm^{-1}) we applied the well-known simplified relation:

$$v_{EM} = \frac{c}{\sqrt{\varepsilon_r}} \quad (4)$$

obtaining a value for ε_r equal to 9.5. By inserting such a value in Eq. (1) and considering $Z_{MAX} = 2$m we obtain a mean electrical conductivity of about 8×10^{-3} Sm^{-1} i.e. a mean resistivity of about 125 Ωm for the first 2 m below the topographic surface, which is a value comparable with the ones obtained with both ERT and FDEM methods (see also the following sections).

In Fig. 5 we can see that there are not apparent lateral changes and no relevant dipping reflectors are imaged, while three high amplitude anomalies (B1, B2, B3) can be detected. B1 is very close to the burrow entrance, while B2 and B3 have no evidence at the surface. In any case anomaly B2 lies within the higher temperature zone observed in the IR data (Fig. 4), corresponding to a local temperature maximum.

Many authors reported that when there is an air-filled volume within a rock or soil there is a polarity inversion on the reflection (or diffraction) related to its top (e.g. Chlaib et al., 2014, just to refer to a paper focusing on embankments). In our case such inversion is not apparent, even possible. Such behavior can be explained considering that tunnels dug by animals are by nature irregular and subsequently they produce different interfering signals preventing a clear phase assessment. Moreover, all the detected anomalies lie very close to the direct GPR arrivals (air and ground waves) making further complicated to evaluate their actual first phase polarity. Oh the other hand, it is interesting to notice that similar signals are not detected for instance in the external flank of the levee and this is in agreement with the fact that digging animals usually prefer to excavate the softer part of the embankment, which is the closest to the riverside (Chlaib et al., 2014).

4.3. FDEM and ERT

The previously described results are confirmed by the FDEM data analysis. Fig. 6 provides an example of FDEM profiles: one crossing the known burrow entrance, and the other parallel to the previous one and located 2.5 m apart. In the zone of the burrow entrance there is a high resistivity anomaly with values exceeding 250 Ωm showing a lateral extension of about 15 m. Just above to this zone the resistivity has a range between 5 and 20 Ωm, values which are never recorded close to the surface in any other portion of the surveyed area. We interpreted such values as due to a discontinuous metallic net put just below the surface in order to limit the digging by animals after a previous intervention dating back to 2015 (AIPo, personal communication). Such obstacle did not prevent the digging of new burrows: the known entrance here described was detected few weeks before the first survey. The vertical resistivity trend in the other portions of the levee is quite homogeneous with values always decreasing from the surface; we conventionally interpreted values below 25 Ωm as saturated materials, marking the 25 Ωm isoresistivity line as the water table (WT).

4.4. Data integration

We further integrated all the data in order to obtain a cross-validation and to get additional and more constrained information about

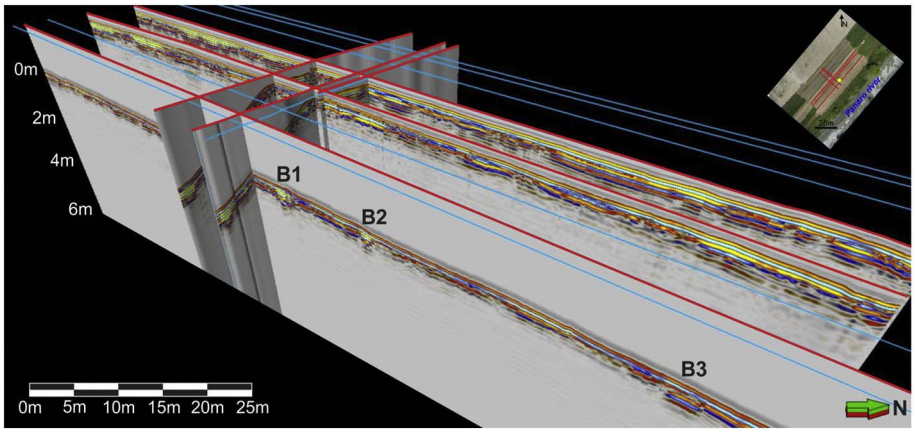

Fig. 5. 3D view of some of the GPR profiles acquired in Survey-1. B1 is an anomaly close to the entrance of the burrow, while B2 and B3 are two other possible tunnels excavated by animals. See text for further details.

the subsurface. The open source software QGIS was used to implement a Geographic Information System (GIS) containing not only the locations of all the acquired data but also the DSM data obtained by the remote sensing photogrammetry, the targets as interpreted and detected from the different geophysical techniques, and the borehole stratigraphies. In detail, while IR anomalies have been manually positioned within the GIS, GPR interpretation has been directly exported from the interpretation software Petrel®. Both ERT and FDEM anomalies have been mapped on the inverted data trying to follow the highest resistivity gradient (even if this procedure is somehow subjective) and then inserted within the GIS.

By comparing the FDEM results with the already reported GPR ones, we find an almost perfect matching. In fact, B1 and B2 anomalies are both inside the highest resistivity zone (also characterized by higher

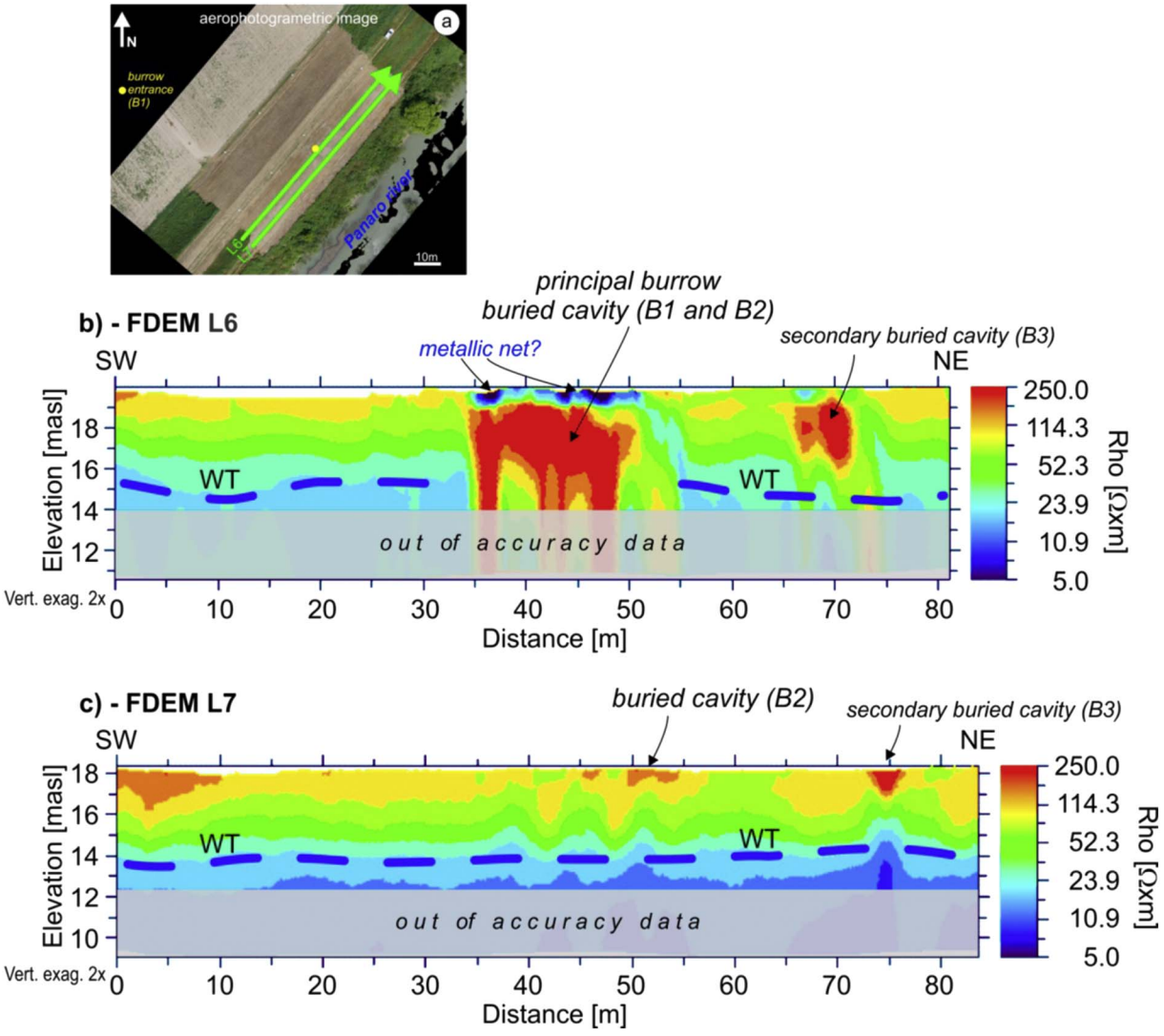

Fig. 6. FDEM results. a) Location map of the two FDEM profiles shown in b) and c); b) inverted resistivity profile L6 across the main entrance of the burrow; c) inverted resistivity profile L7 parallel to L6 and located 2.5 m apart. B1, B2, B3 are burrows or possible burrows as labeled in Fig. 5. WT is the interpreted water table (see also Fig. 7).

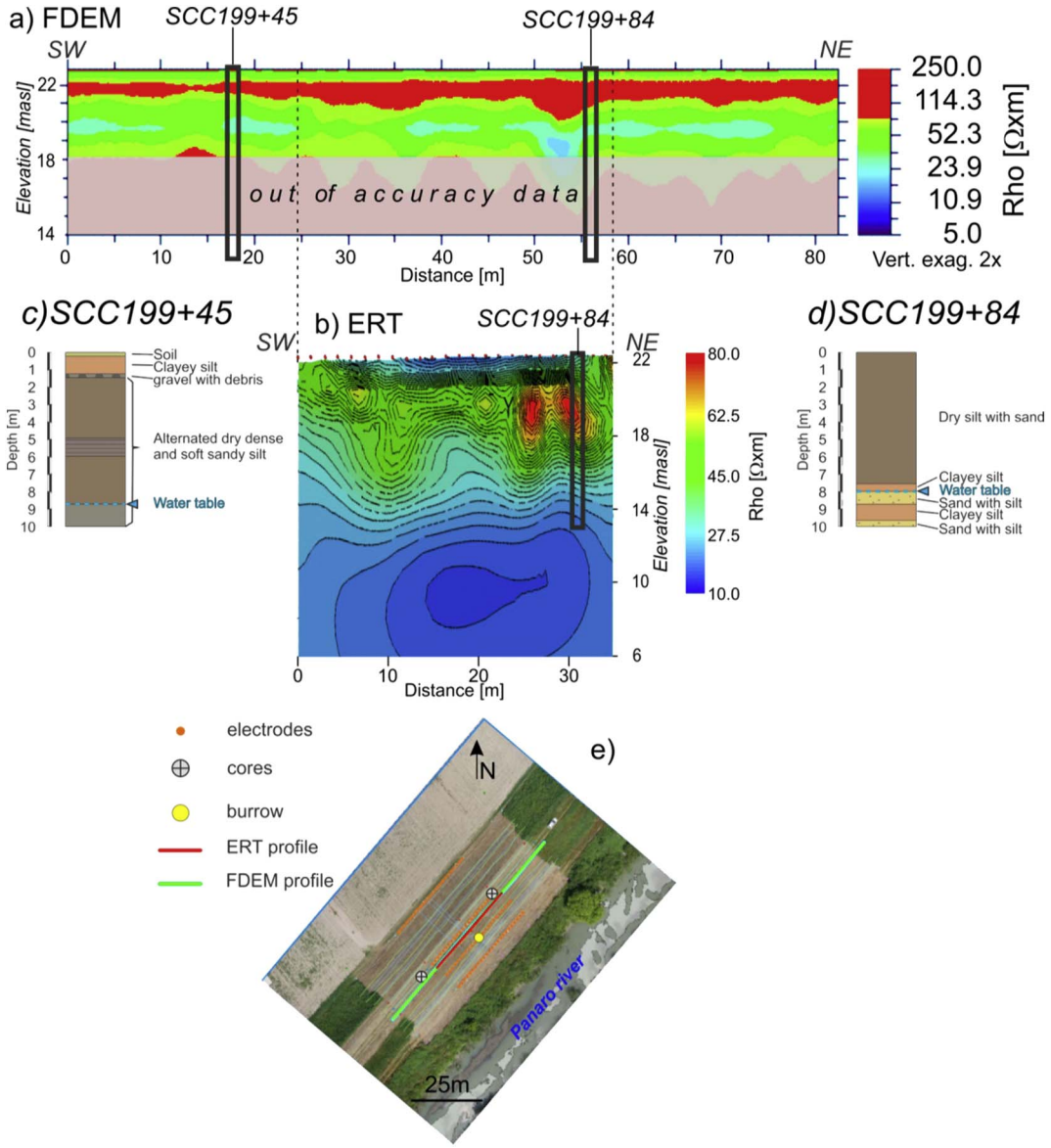

Fig. 7. Comparison between FDEM (a); ERT (b); core logs (c, d) along the same profile. In e) the location map of the shown data is provided. During the digging of borehole SCC 199 + 45 two voids were detected from 5.70 m to − 5.90 m and − 6.10 m to − 6.30 m.

temperature by the IR survey). Moreover, anomaly B3 toward North-East also corresponds to a high resistivity zone. The two parallel profiles shown in Fig. 6b and c are quite different: while the resistivity anomaly interpreted as due to B1 and B2 is clear only on the uppermost profile (L6), B3 seems to continue toward the base of the levee and it is apparent also on profile L7. The resolution and reliability of the data is rapidly diminished going to increasing depths and below about 5 or 6 m the inverted results are not meaningful.

It is interesting to notice that localized resistivity values above about 200 Ωm obtained after the inversion of FDEM data seem to be always related to underground tunnels due to animal burrows, independently by their depth from the surface, while laterally extended high resistive zones almost parallel to the topography are mainly due to dry sediments containing sand or levels of gravel (Fig. 7). In fact, the cores drilled at the top of the embankment in order to characterize its sedimentological, geotechnical and hydrogeological structure evidenced materials always having a decreasing resistivity trend, mainly due to increasing water saturation in the vadose zone and with the presence of an underlying water table (Fig. 7).

Results obtained by FDEM and ERT are similar, both showing the same resistivity trend, even with different absolute resistivity values (Fig. 7a, b). The smaller range of the ERT measurements, especially with lower maximum values is probably due to a minor resolution of the electrical tomography made with dipoles spaced at least by 1.5 m. On the other hand, the saturated zone and the water table are properly identify only on ERT data, with an high negative resistivity gradient, while the depth of the water table, as measured by the boreholes between 8 and 9 m from the surface is too deep for the FDEM measures set with the frequency and the offsets as in the present case. Lateral resistivity variations can be highlighted by both FDEM and ERT data, but their precise correlation with specific lithologies is not apparent due to the high lateral variability of the building materials of the embankment (Fig. 7c, d).

4.5. Survey-1 and Survey-2 data comparison

Further interesting information can be obtained by comparing the GPR and ERT data acquired in Survey-1 and in Survey-2, being the latter acquired soon after the injection of bentonite cement into the main burrow. In Fig. 8 an example of GPR data comparison is provided.

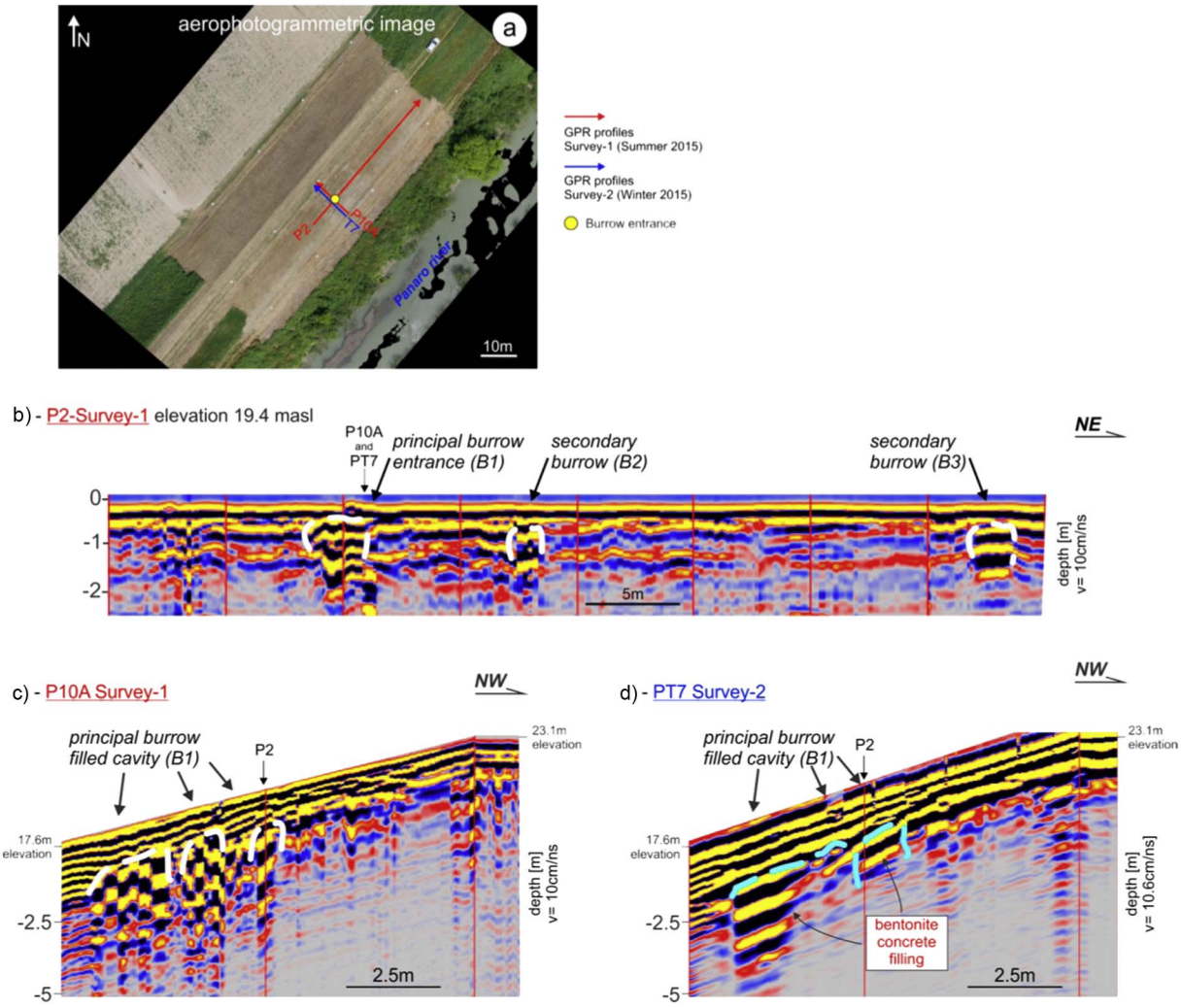

Fig. 8. Comparison of GPR data before (Survey-1) and after (Survey-2) the filling of the burrow with bentonite cement. a) Location map of shown profiles; b) and c) profiles of Survey-1 closest to the main burrow entrance; d) same profile as c) but acquired during Survey-2. All the data shown are migrated. For a better data comparison, please consider that the mean electromagnetic velocity used for the depth conversion slightly increased from Survey-1 to Survey-2 from about 10 cm/ns up to 10.6 cm/ns.

In Fig. 8 one longitudinal (b) and one transversal profile (c) acquired in Survey-1, crossing the principal burrow entrance and crossing each other are shown. On both profiles the main burrow (B1), as well as the other two already described underground possible tunnels (B2 and B3) are imaged by high amplitude reflections/diffractions, with several reverberated phases due to the high electromagnetic contrast between soil and air (see also Fig. 5). The lateral phase behavior is in general chaotic with laterally uncorrelated events having different phases. This is particularly true for B1, which is probably the wider and the most complex burrow made by several interconnected tunnels (see also Fig. 6). The resolution of the 300 MHz GPR antenna is therefore not sufficient to image the details of such burrow, which is on the other hand very apparent on both longitudinal and transversal profiles. By comparing the same profile before (Fig. 8c) and after (Fig. 8d) the bentonite filling we can notice relevant changes in the signature of the GPR signal. The main variations are located in an about 4 m wide zone centered around the burrow entrance. The filling produced smoothed reflections (without or with only minor diffractions) showing high lateral phase continuity and high reflectivity. This behavior can be explained considering that the cement slurry was injected under pressure and was able to fill almost all the pre-existing cavities, so creating a rather uniform zone on a quite wide area. This way the lateral changes due to the air-filled tunnels are obliterated and the reflections become more continuous. This is even clearer by analyzing phase-related attributes like the instantaneous phase or the cosine of instantaneous phase.

Relevant differences can be highlighted also by considering the ERT data of Survey-1 and Survey-2 (Fig. 9).

The analysis of both row and inverted data of the two surveys showed that the average “background” resistivity was quite similar, even if in Survey-2 the calculated mean resistivity was equal to 21 Ωm, while in Survey-1 was 30 Ωm. This behavior is probably due to a higher moisture content during Survey-2 (i.e. in Winter); in fact such a difference is more detectable in the shallower layers where the effect of rainfall is bigger.

Survey-1 evidenced resistivity values higher than about 40 Ωm in a 15 to 20 m wide zone, similar to the one observed in FDEM data (Fig. 6), which can be associated to interconnected air-filled cavities. After the cement filling (Survey-2, Fig. 9b) such zone almost disappears. In fact, while close to the surface some low resistivity areas are nearly unchanged, below there are values similar to the background instead of the previous high resistivity, except toward the NE border of the profile. On the other hand, where the high resistivity anomalies were not detected during Survey-1 the values in the correspondent profiles acquired during Survey-2 are basically unchanged. This is even more apparent when considering the resistivity difference between Survey-1 and Survey-2 (Fig. 9c). After the burrow filling, we can expect smaller resistivity values due to the cement inside the previously air-filled

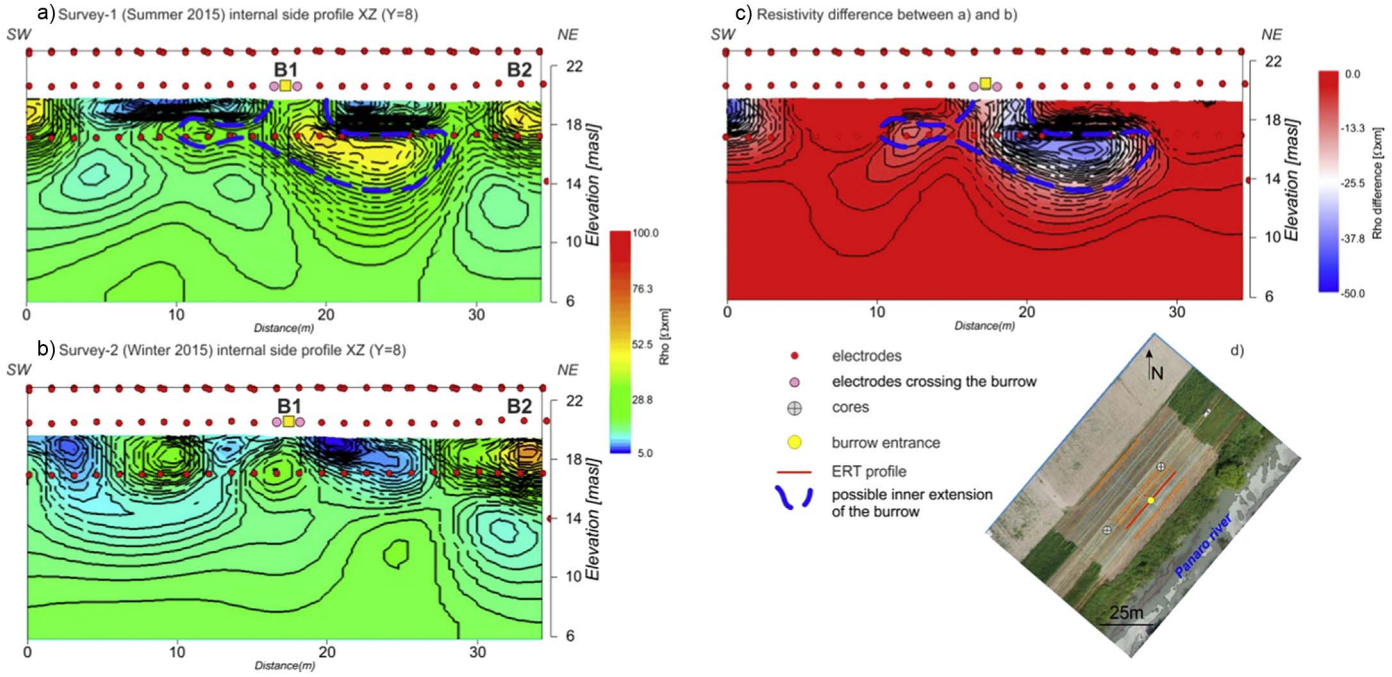

Fig. 9. ERT profiles extracted from the resistivity volume across the main burrow. a) profile xz of Survey-1 just below the visible burrow entrance, where the highest resistivity values (> 40 Ωm) are mostly inside the blue dashed line depicting the possible underground extension of the buried cavity; b) profile xz of Survey-2 along the same location as in a): a resistivity lowering is apparent especially in the first 3 m below the surface; c) difference between a) and b); d) location map of the shown profiles. (For interpretation of the references to colour in this figure legend, the reader is referred to the web version of this article.)

Table 1
Average dimensions and shapes of badger setts (after: Roper, 1992a, b; Nichol et al., 2003; Roper, 2010).

Tunnel	Shape	Circular and/or elliptical
	Width	0.3 m
	Length	5–10 m
	Height	0.2 m
	Inclination	45° downwards
	Depth	0.5 to 2.5 m above groundwater level
Chamber	Shape	Elliptical
	Width	0.6 m
	Length	0.4 m
	Height	0.4 m

cavities. This is confirmed by the data, which shows a resistivity lowering up to about 50 Ωm in a well-defined 15 m wide zone centered below the main burrow entrance, while in the other investigated area the resistivity shows a moderate decrease, due to the different moisture content during the two surveys, as already pointed out. Only few other small zones exhibit a relevant resistivity lowering (for instance the one at the NW border on Fig. 9c), but they seem to be more related to inaccuracies of the inversion models rather than to actual subsurface structures. At the opposite, unchanged high resistivity portions (B2 in Fig. 9) seem to be realistic, meaning that the bentonite cement was not able to fill all the tunnels branches possibly because some of the air-filled network was not actually interconnected or it is at higher elevation.

5. Discussion

The integration of geophysical data allows to highlight the presence of an about 15 m wide burrow developing from the active known entrance, as well as to detect other tunnels in the body of the levee. As in the area of Finale E. a total of 21 European badgers and porcupines were caught and delocalized in the last one year and a half, it is assumed that the known and the detected burrows were created by these animals.

The geometry of burrows depends on the animals: European badgers and crested porcupines build similar systems, which are often shared with red foxes. European badgers build complex burrow systems called setts, which are generally located at low altitude and in steep slopes, with vegetation cover and above the groundwater table (Byrne et al., 2012). The setts are dug in dry loam, sandy and clayey soils, relatively easy terrains to be excavated (Kruuk, 1978; Reddi et al., 2008). The setts are composed by several tunnels and chambers and their size and complexity are controlled by the function, the soil type and the age. The central part is constituted by a main sett with several entrances (from 1 up to 50), while secondary setts can be located from 50 m up to 150 m away. As an example, Roper (2010) reports of 3 setts, one of which had 38 entrances, 78 chambers, 360 m long tunnel network and a total volume of 25 m^3 (Table 1). The badger burrows are tunnels with semi-circular or elliptical shape, about 0.20 m high and 0.30 m wide (Nichol et al., 2003). The tunnels start with an inclination of 40–45° then can run horizontally. The chambers can be located at different depths at the end of the burrows, 5–10 m away from the entrance, or can be a simple widening of the tunnels. Some tunnels can be directed upslope to facilitate ventilation, while other tunnels might be directed downslope for drainage purposes.

The levee of the Panaro River, in fact, appears as an ideal environment for the presence of badgers, porcupines and foxes. The embankment is around 8 m high, and is covered by grass. Shrubs and small trees grow at the base of the waterside slope. Few houses are located in the vicinity of the embankment, while the main road is > 100 m far away. The soil is composed of silt with sand, and is dry during most of the year at least down to about 6–8 m depth (Figs. 2 and 3).

By integrating all the available data we produced a 3D model of the main burrow, which was further materialized by using a 3D printing device (Fig. 10). It is quite obvious that there are unavoidable inaccuracies in the shape and in the dimension of such result, but both dimensions and shape of the sett are well in accordance with the expected ones. Moreover, it is interesting to notice that the volume obtained is of about 30.4 m^3, with the same order of magnitude of the quantity of bentonite cement (19 m^3) injected into the burrow. The

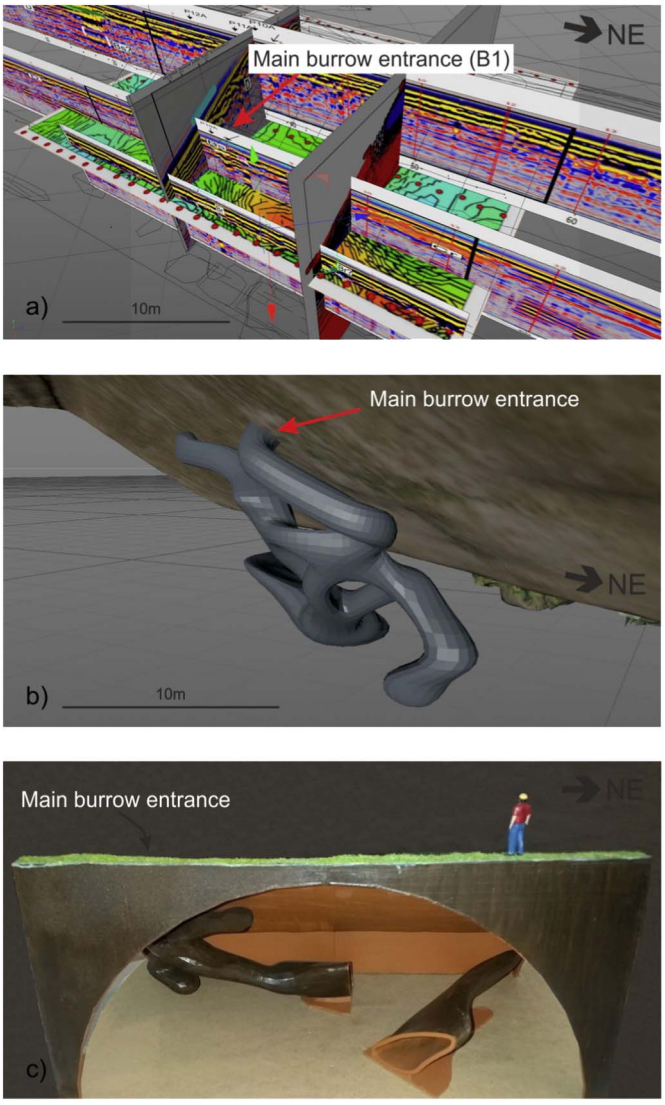

Fig. 10. a) Geophysical data integration; b) rendering of the main burrow obtained integrating all the geophysical data with the evidences of video inspections;c) model of the burrow (reproduction scale 1:50) made with a 3D printer by using the data as in b).

latter value is smaller than the volume estimated by the integrated geophysical data probably because some branches of the burrow were not completely filled, as also suggested by the previously discussed ERT data comparison (B2 in Fig. 9). Moreover, the resulting shape is comparable with real setts as documented by several studies (Roper, 1992a, b; Nichol et al., 2003; Roper, 2010), both in terms of tunnels and chambers dimensions and geometry. The depth reached by the sett is equal to about 4 m, which is above the groundwater table depth and the river level.

Considering that: the levee has an almost constant cross section with an area of about 125 m^2; the length of the main burrow as imaged by the integrated geophysical techniques is approximately equal to 15 m; its estimated volume is, as already pointed out of 30.4 m^3, we deduce that the main burrow occupies about 1.6% of the total volume of the investigated stretch of the levee. Such estimations may be very important in the deterministic and statistical assessment of embankment stability where voids are observed or expected. Of course, relatively small but interconnected macro-pores can on the one hand diminish the average strength of the materials and, on the other hand, represent a preferential way for water infiltration also depending on their position with respect to the water level in the river.

Based on the results, some considerations can be drawn on each single technique and the integrated approach.

The IR data collected both during the day and nighttime are not only able to detect the known burrow entrance but, even more important, to suggest the presence of underground air-filled tunnels. However, from our experience it is not so straightforward to correlate a thermal anomaly to an underground structure, since it can be partially produced by reworked materials at the surface or to different/lower vegetation cover. In any case the comparison between IR and other geophysical data (especially ERT and FDEM) seems to suggest that the geometry of the thermal anomalies gives some indications about the presence of tunnels and can be a practical and relatively rapid tool for monitoring activities and to plan interventions and maintenance of the embankment.

The use of pseudo 3D GPR volumes and 3D inversion of ERT and FDEM data can be essential when the aim is not only to detect a buried burrow but also to infer its extension, shape and volume. Although with different resolution levels, electrical, and both low and high frequency electromagnetic techniques are able to detect and image the burrow below the surface. From the logistical point of view all the tested methods have some constrains. The IR can provide good results only when bushes and trees are absent or at least they are without leaves and the grass is short enough. The GPR is quite versatile, but needs some adapting and special cares especially to record longitudinal profiles along the flanks of the levee. A simple plastic support mounted on a kart with wheels and connected with robust ropes seems to work quite well providing good performances in terms of time productivity (about 1.5 km/h) and average data quality. A similar result can be achieved with FDEM devices. In fact, a plastic casing linked with the GPS antenna can make the data acquisition easier even along the dipping flanks, providing at the same time high data positioning accuracy. ERT survey suffers less logistical limitation since it can be tailored even when there are obstacles on the surface (like, for instance, trees). The resistance between the electrodes and the terrain, carefully checked and eventually minimized before each acquisition, did not produce severe coupling limitations even during the summer survey. The main constrain of the ERT, especially in 3D mode, is the time required to set the electrodes and to acquire the data, reaching in the present case a total time of about 4–5 h. So it is impossible to propose extensive ERT measurements to detect unknown burrows in an embankment, while GPR and FDEM measurements perform better, both requiring about one hour to collect data along 1–2 km.

All the measures can be done in any season. Better GPR performances can be obtained during the driest period when the penetration depth can reach the maximum, while it would be preferable to collect ERT data when the soil is wet. In fact, the resistance between electrodes and soil is minimized and the contrast between air and sediments is higher. We does not repeated the TDEM survey but we guess that it could perform equally well in different periods, being probably from this point of view the most flexible method.

The test made after the filling of the burrow allows us to distinguish relevant differences between air- and cement-filled cavities by using both GPR and ERT. From the examples provided (Figs. 8 and 9) we can conclude that the resistivity changes are probably more apparent than the GPR signal variations, even if a careful analysis of the phase behavior of the electromagnetic signal allows affordable and quite clear results to be obtained.

6. Conclusions

The results of the integrated multi-technique approach allowed the known badger burrow as well as two other tunnels to be imaged, providing specific guidelines for the best integrated strategy to detect and characterize such kind of structures in a fluvial levee. The position, the distribution, the volume and the complexity of the network were described well in accordance with the expected dimension and shape of the sett.

Table 2
Synthesis of applicability, strengths and limitations for APT, IR, GPR, ERT and FDEM techniques for burrows detection and imaging in fluvial embankments.

Method	Accuracy Resolution	Suitability for large scale surveys	Strengths	Limitations	Applicability
APT	Very high	Yes	High acquisition rate; centimetric precision	Constrains in the use of UAV	High
IR	High	Yes	High acquisition rate; high spatial resolution	Presence of dense vegetation; dependency on the acquisition time	High
GPR	High	Yes	Accurate imaging	Limited maximum achievable penetration depth	Medium
ERT	Low/medium	No	Acquisition scheme adaptable as a function of logistics/expected targets	Low acquisition rate; resolution strongly decreases with depth	High
FDEM	Low/medium	Yes	High acquisition rate	Resolution strongly decreases with depth/ limited vertical resolution	High

In Table 2 we summarize strengths and limitations of each tested methodology on the base of the lesson learned by the present research. Besides some general and peculiar characteristics of each technique, it is important to remark that each of them is strongly site- and target-dependent and therefore it is practically impossible to predict the performances before doing some preliminary tests in the field. In any case, we found that while GPR is very effective and accurate to detect and image the top of subsurface burrows chambers and tunnels, ERT and FDEM are both useful to estimate the burrow volume, especially when integrated 2D and 3D acquisitions are performed, as in the present case. IR is a high potential technique which should be further tested and exploited in the near future, even for large scale surveys, while the APT is a fast remote sensing technique, allowing the reconstruction of the topography with centimetric accuracy, which is mandatory to evaluate both the actual geometry of the levee and to position the subsurface targets with high precision.

The construction of the resulting 2D/3D geological models by integrating different techniques is essential to assess and eventually monitor the integrity of representative sections of river embankments with different defects.

The proposed approach can advance our knowledge of embankments in space and time, so that effective remedial actions in flood risk and wildlife management can be identified. In this sense, the 3D physical model can be useful for end users, decision makers, as well as for untrained people to get a better focus on the problem, which is always the preliminary step to any risk management procedure toward the evaluation of the best operational strategies. Further researches could be addressed to collect IR data from a dedicated airborne-mounted device and to assess the stability of disturbed flood control structures under different boundary conditions.

Acknowledgments

The authors wish to acknowledge the support from AIPo, for giving the permission to use the data and Artificio Digitale snc who made the 3D model of the burrow. We further acknowledge Schlumberger through the University of Trieste Petrel® interpretation package academic grant. Thanks to G. Tedesco e A. Gobbi for the support during field work and to D. Castaldini for the discussion about Panaro River geomorphological features.

We further acknowledge two anonymous reviewers for their fruitful suggestions.

Appendix A. Supplementary data

Supplementary data to this article can be found online at http://dx.doi.org/10.1016/j.enggeo.2017.06.017.

References

Anderson, M.P., 2005. Heat as a groundwater tracer. Ground Water 43, 951–968.
Bayoumi, A., Meguid, M.A., 2011. Wildlife and safety of earthen structures: a review. J. Fail. Anal. Prev. 11 (4), 295–319. http://dx.doi.org/10.1007/s11668-011-9439-y.
Branham, K.L., Steeples, D.W., 1988. Cavity detection using high-resolution seismic reflection methods. Miner. Eng. 40, 115–119.
Busato, L., Boaga, J., Peruzzo, L., Himi, M., Cola, S., Bersan, S., Cassiani, G., 2016. Combined geophysical surveys for the characterization of a reconstructed river embankment. Eng. Geol. 211, 74–84.
Butler, D.K., 1984. Microgravimetric and gravity gradient techniques for the detection of subsurface cavities. Geophysics 49, 1084–1096.
Butler, J., Roper, T.J., Clark, A.J., 1994. Investigation of badger (*Meles Meles*) setts using soil resistivity measurements. J. Zool. 232 (3), 409–418.
Byrne, A.W., Sleeman, D.P., O'keeffe, J., Davenport, J., 2012. The ecology of the European Badger (*Meles Meles*) in Ireland: a review. Biol. Environ. Proc. R. Ir. Acad. 112.
Cannarozzo, R., Cucchiarini, L., Meschieri, W., 2012. Fotogrammetria in: Misure, rilievo, progetto, Zanichelli Ed.; (Bologna, 33pp).
Castaldini, D., Ghinoi, A., 2008. Recent morphological changes of the River Panaro (Northern Italy). Il Quaternario, Ital. J. Quat. Sci. 21 (1B), 267–278.
Chlaib, H.K., Mahdi, H., Al-Shukri, H., Su, M.M., Catakli, A., Abd, N., 2014. Using ground penetrating radar in levee assessment to detect small scale animal burrows. J. Appl. Geophys. 103, 121–131.
Cho, I., Yeom, J., 2007. Crossline resistivity tomography for the delineation of anomalous seepage pathways in an embankment dam. Geophysics 72, G31–G38.
CIRIA, 2013. PUB C731 International Levee Handbook. CIRIA, London (1348pp).
D'Alpaos, L., Brath, A., Fioravante, V., Gottardi, G., Mignosa, P., Orlandini, S., 2014. Report on the causes of the levee failure occurred on the Secchia River at San Matteoon January 19, 2014 (In Italian), Final Report Released on July 9, 2014. Commission formed by the governor of Regione Emilia-Romagna, Bologna, Italy.
Daniels, D., 2004. Ground Penetrating Radar. In: vol. 15 of IEE Radar, Sonar, Navigation and Avionics Series, 2nd edition. The Institution of Electrical Engineers, MPG Books (300pp., ISBN: 0-85296-862-0).
Deidda, G.P., Ranieri, G., 2005. Seismic tomography imaging of an unstable embankment. Eng. Geol. 82 (1), 32–42.
Deitchman, R.S., Loheide II, S.P., 2009. Ground-based thermal imaging of groundwater flow processes at the seepage face. Geophys. Res. Lett. 36, L14401.
Di Prinzio, M., Bittelli, M., Castellarin, A., Rossi Pisa, P., 2010. Application of GPR to the monitoring of river embankments. J. Appl. Geophys. 71 (2–3), 53–61.
FEMA Federal Emergency Management Agency, 2005. Technical Manual for Dam Owners: Impacts of Animals on Earthen Dams. FEMA Report 473 Federal Emergency Management Agency, Washington, DC.
Forte, E., Pipan, M., 2009. Correzione topografica integrativa di dati GPR: considerazioni teoriche e applicazione a dati reali. In: Extended abstract of the 28th GNGTS congress, Trieste, 16-19 November 2009, pp. 700–704.
Forte, E., Pipan, M., Casabianca, D., Di Cuia, R., Riva, A., 2012. Imaging and characterization of a carbonate hydrocarbon reservoir analogue using GPR attributes. J. Appl. Geophys. 81, 76–87. http://dx.doi.org/10.1016/j.jappgeo.2011.09.009.
Jones, G., Sentenac, P., Zielinski, M., 2014. Desiccation cracking detection using 2-D and 3-D electrical resistivity tomography: validation on a flood embankment. J. Appl. Geophys. 106, 196–211.
Jol, H.M. (Ed.), 2009. Ground Penetrating Radar: Theory and Applications. Elsevier Science, The Netherlands (524pp., ISBN: 978-0-444-53348-7).
Kaufman, A.A., Keller, G.V., 1983. Frequency and Transient Soundings. Elsevier, Amsterdam (685pp).
Kinlaw, A.E., Conyers, L.B., Zajac, W., 2007. Use of ground penetrating radar to image burrows of the gopher tortoise (Gopheruspolyphemus). Herpetol. Rev. 38 (1), 50–56.
Kruuk, H., 1978. Spatial organization and territorial behaviour of the European badger (*Meles Meles*). J. Zool. 184, 1–19.
Loperte, A., Soldovieri, F., Palombo, A., Santini, F., Lapenna, V., 2016. An integrated geophysical approach for water infiltration detection and characterization at Monte Cotugno rock-fill dam (southern Italy). Eng. Geol. 211, 162–170.
Lorenzo, J.M., Hicks, J., Vera, E.E., 2014. Integrated seismic and cone penetration test observations at a distressed earthen levee: Marrero, Louisiana, U.S.A. Eng. Geol. 168, 59–68.
McNeill, J.D., 1980. Electromagnetic Terrain Conductivity Measurement at Low Induction Numbers. Technical note TN-6 Geonics Limited, Mississauga, Ontario, Canada (13pp).
Monteiro Santos, F.A., 2004. 1-D laterally constrained inversion of EM34 profiling data. J. Appl. Geophys. 56, 123–134.
Monteiro Santos, F.A., Triantafilis, J., Bruzgulis, K., 2011. A spatially constrained 1D inversion algorithm for quasi-3D conductivity imaging: application to DUALEM-421 data collected in a riverine plain. Geophysics 76 (2), B43–B53. http://dx.doi.org/10.1190/1.3537834.

Nichol, D., Lenham, J.W., Reynolds, J.M., 2003. Application of ground-penetrating radar to investigate the effect of badger setts on slope stability at St Asaph Bypass, North Wales. Q. J. Eng. Geol. Hydrogeol. 36 (2), 143–153. http://dx.doi.org/10.1144/1470-9236/2002-42.

Niederleithinger, E., Weller, A., Lewis, R., 2012. Evaluation of geophysical techniques for dike inspection. J. Environ. Eng. Geophys. 17 (4), 185–195.

Oldenburg, D.W., Li, Y., 1999. Estimating depth of investigation in dc resistivity and IP surveys. Geophysics 64, 403–416.

Orlandini, S., Moretti, G., Albertson, J.D., 2015. Evidence of an emerging levee failure mechanism causing disastrous floods in Italy. Water Resour. Res. 51 (10), 7995–8011. http://dx.doi.org/10.1002/2015WR017426.

Panthulu, T.V., Krishnaiah, C., Shirke, J.M., 2001. Detection of seepage paths in earth dams using self-potential and electrical resistivity methods. Eng. Geol. 59, 281–295.

Perri, M.T., Boaga, J., Bersan, S., Cassiani, G., Cola, S., Deiana, R., Simonini, P., Patti, S., 2014. River embankment characterization: the joint use of geophysical andgeo-technical techniques. J. Appl. Geophys. 110, 5–22.

Reddi, N., Etherington, T.R., Wilson, G., Montgomery, W.I., 2008. Badger Survey of Northern Ireland 2007/2008. Report prepared by Quercus and Central Science Laboratory for the Department of Agriculture & Rural Development (DARD), Northern Ireland, UK.

Reynolds, J.M., 1997. An Introduction to Applied and Environmental Geophysics. John Wiley and Sons, England (796pp., ISBN: 0-471-96802-1).

Richards, K.S., Reddy, K.R., 2010. New approach to assess piping potential in earth dams and levees. ASCE NEWS 51 (6), A1–A10.

Roper, T.J., 2010. Badger. Collins New Naturalist Library, Book. 114 (416pp).

Roper, T.J., 1992a. The structure and function of badger setts. J. Zool. Lond. 227, 691–698.

Roper, T.J., 1992b. Badger Mele smeles setts-architecture, internal environment and function. Mammal Rev. 22 (1), 43–53.

Samyn, K., Mathieu, F., Bitri, A., Nachbaur, A., Closset, L., 2014. Integrated geophysical approach in assessing karst presence and sinkhole susceptibility along flood-protection dykes of the Loire River, Orléans, France. Eng. Geol. 183, 170–184.

Sentenac, P., Jones, G., Zielinski, M., Tarantino, A., 2012. An approach for the geophysical assessment of fissuring of estuary and river flood embankments: validation against two case studies in England and Scotland. Environ. Earth Sci. http://dx.doi.org/10.1007/s12665-012-2026-z.

Sheng Huoo, N., Ching-Kuan, C., Hong-Ming, L., 2002. Application of ground penetrating radar on the void-detection in levee. Proc. Int. J. Offshore Polar Eng.

Taccari, M.L., 2015. Study upon the Possible Influence of Animal Burrows on the Failure of the Levee of san Matteo along the Secchia River. MSc Thesis Civil Engineering Geo-Engineering Section, Civil Engineering and Geosciences, TU Delft (138 pp).

Ursin, B., 1983. Review of elastic and electromagnetic wave propagation in horizontally layered media. Geophysics 48 (8), 1063–1081.

Xu, X., Zeng, Q., Li, D., Wu, J., Wu, X., Shen, J., 2010. GPR detection of several common subsurface voids inside dikes and dams. Eng. Geol. 111 (1–4), 31–42.

Zhao, W.K., Forte, E., Pipan, M., Tian, G., 2013. Ground Penetrating Radar (GPR) attribute analysis for archaeological prospection. J. Appl. Geophys. 97, 107–117. http://dx.doi.org/10.1016/j.jappgeo.2013.04.010.